Cell Death and Differentiation (2009) 16, 1332–1343

www.nature.com/cdd

IL-17 stimulates the proliferation and differentiation of human mesenchymal stem cells: implications for bone remodeling

H Huang[1], HJ Kim[1], E-J Chang[1], ZH Lee[1], SJ Hwang[1,2], H-M Kim[1], Y Lee*[,1] and H-H Kim*[,1]

Interleukin-17 (IL-17) is a cytokine secreted primarily by T_H-17 cells. Although IL-17 is primarily associated with the induction of tissue inflammation, the other biological roles of IL-17, including non-immune functions, have yet to be thoroughly explored. Here, we report that T-cell-produced IL-17 can induce proliferation of human bone marrow-derived mesenchymal stem cells (hMSCs) in a manner dependent on the generation of reactive oxygen species (ROS). Rac1 GTPase and NADPH oxidase 1 (Nox1) are activated by IL-17 to produce ROS, which in turn stimulates hMSC proliferation. The activation of the MEK-ERK pathway is also crucial for IL-17-dependent hMSC proliferation. TRAF6 and Act1 are required to activate Nox 1 and to phosphorylate MEK on IL-17 stimulation. Interestingly, IL-17 not only accelerates the proliferation of hMSCs, but also induces their migration, motility, and osteoblastic differentiation. Furthermore, IL-17 induces the expression of M-CSF and receptor activator of NF-κB ligand (RANKL) on hMSCs, thereby supporting osteoclastogenesis both *in vivo* and *in vitro*. On the basis of these results, we suggest that IL-17 can function as a signal to induce extensive bone turnover by regulating hMSC recruitment, proliferation, motility, and differentiation.
Cell Death and Differentiation (2009) **16,** 1332–1343; doi:10.1038/cdd.2009.74; published online 19 June 2009

The interleukin-17 (IL-17) cytokine family is a family of proinflammatory cytokines comprising six members: IL-17A to IL-17F.[1,2] IL-17 is thought to be involved in tissue inflammation by stimulating the release of other proinflammatory cytokines and inducing neutrophil chemotaxis.[1] Moreover, IL-17 has been associated with various human diseases such as systemic lupus erythematosus, asthma, rheumatoid arthritis, and allograft rejection.[3–6] Recently, T_H-17 cells derived by IL-23 were identified as a novel subset of $CD4^+$ effector T cells that produce IL-17A and IL-17F.[7] In addition, various cellular sources of IL-17 including $CD4^+$ memory T cells, $CD8^+$ memory T cells, neutrophils, and eosinophils have been identified.[8–11]

Recent studies have shown that IL-17 also affects the functions of non-immune cells. IL-17 has been shown to induce the expression of receptor activator of NF-κB ligand (RANKL) on osteoblasts.[5] Furthermore, the level of IL-17 in the synovia of rheumatoid arthritis patients is particularly high, suggesting that IL-17 may play a role in this bone-destructive disease.[5] RANKL, expressed mainly on osteoblasts and T cells, supports the differentiation of osteoclasts, the bone-resorbing cells of macrophages/monocyte origin.[12] In addition, IL-17-producing T_H-17 cells were identified as a RANKL-expressing T-cell subset, suggesting a pivotal role of these cells in the regulation of bone homeostasis.[13] In pilot experiments to assess the role of IL-17 in the bone microenvironment, we discovered that IL-17 stimulated the proliferation of human mesenchymal stem cells (hMSCs). MSCs are pluripotent progenitor cells that contribute to the regeneration of mesenchymal tissues, including bone, adipose tissue, cartilage, muscle, ligament, tendon, and stroma.[14] Although IL-17 was shown to increase the formation of fibroblast-like colonies from bone marrow cells,[15] the exact identity of those colony-forming cells and the detailed mechanism by which IL-17 stimulates proliferation of those cells has not yet been elucidated. In this study, we delineated the IL-17-dependent signaling pathways that lead to increased proliferation of hMSCs using a defined population of cells, and explored the role of IL-17 in hMSC differentiation and function. We show that the generation of reactive oxygen species (ROS) is crucial for IL-17-stimulated hMSC proliferation. Furthermore, our results suggest that IL-17 also stimulates the migration, motility, and osteoblastic differentiation of hMSCs. In addition, IL-17 induces the expression of M-CSF and RANKL on hMSCs, thereby stimulating osteoclastogenesis, both in *in vitro* coculture and in *in vivo* implant experiments. These results suggest a novel role of IL-17 in the regulation of hMSC function for the maintenance of bone homeostasis as well as the pathogenesis of bone-destructive diseases.

[1]Department of Cell and Developmental Biology, BK21 and DRI, Seoul National University School of Dentistry, Seoul 110-749, Korea and [2]Department of Oral and Maxillofacial Surgery, BK21 and DRI, Seoul National University School of Dentistry, Seoul 110-749, Korea
*Corresponding authors: Y Lee, Department of Cell and Developmental Biology, Seoul National University School of Dentistry, 28 Yongeon-Dong, Chongno-Ku, Seoul 110-749, Korea. Tel: +82 2 740 8738; Fax: +82 2 765 8656; E-mail: yklee@snu.ac.kr
or H-H Kim, Department of Cell and Developmental Biology, Seoul National University School of Dentistry, Seoul, 110-749, Korea. Tel: +82 2 740 8686; Fax: +82 2 765 8656; E-mail: hhbkim@snu.ac.kr
Keywords: IL-17; human mesenchymal stem cells; osteoblast; proliferation
Abbreviations: ALP, alkaline phosphatase; DCFH-DA, dichlorofluoroscein diacetate; hMSC, human bone marrow-derived mesenchymal stem cell; NAC, N-acetylcysteine; Nox, NADPH oxidase; RANKL, receptor activator of NF-κB ligand; ROS, reactive oxygen species
Received 15.9.08; revised 27.4.09; accepted 14.5.09; Edited by R De Maria; published online 19.6.09

Results

IL-17 stimulates hMSC proliferation, osteoblastic differentiation, and motility. In the bone microenvironment, interactions between T cells, osteoclasts, and osteoblasts play crucial roles in determining bone homeostasis. Interestingly, rheumatoid arthritis synovium is rich in IL-17, which stimulates osteoclast-mediated bone destruction through upregulation of RANKL expression on osteoblasts.[5] As MSCs have the potential to differentiate into osteoblasts, we focused on the effects of IL-17 on hMSCs. First, we examined the characteristics of hMSCs used in our experiments. Both primary hMSCs and Cambrex hMSCs exhibited the potential to differentiate into osteoblasts, adipocytes, and chondrocytes (Supplementary Figure 1). Furthermore, both primary hMSCs and Cambrex MSCs expressed hMSC markers such as CD73, CD90, CD105, and CD166 (Supplementary Figure 2). Thus, we used these cells in further experiments to define the role of IL-17 in hMSCs. To date, five members of the IL-17 receptor family have been identified based on sequence similarity to the originally described IL-17Ra.[1,8] Reverse transcription (RT)-PCR analysis showed that the hMSCs expressed all five members of the IL-17 receptor family, although expression of IL-17Re was relatively low (Figure 1a). The surface expression of IL-17Ra was confirmed by fluorescence-activated cell sorting (FACS) analysis (Figure 1b). To test whether IL-17 can stimulate hMSC proliferation, we cultured primary or Cambrex hMSCs in the presence of IL-17 and assessed the amount of bromodeoxyuridine (BrdU) incorporation (Figure 1c and Supplementary Figure 3a). When hMSCs were treated with 50 ng/ml IL-17 for up to 8 days, BrdU uptake was significantly increased, suggesting that IL-17 promotes proliferation of these cells. Increasing concentrations of IL-17 enhanced the proliferation of hMSCs, with 5 ng/ml of IL-17 showing a significant stimulatory effect (Supplementary Figure 3b). Although the ligand specificity of the IL-17 receptor family has yet to be clarified, it is likely that IL-17 signaling is mediated primarily by IL-17Ra.[1] Thus, we evaluated the involvement of IL-17Ra in the IL-17-dependent proliferation of hMSCs. Although control IgG had no effect, anti-IL-17Ra neutralizing antibody almost completely negated the effect of IL-17 on the proliferation of Cambrex MSCs (Figure 1d) and primary hMSCs (Supplementary Figure 3a). When cultured with IL-17, significantly higher numbers of hMSCs became alkaline phosphatase (ALP) positive compared with cells grown in media alone, suggesting that IL-7 is a potent inducer of osteoblastic differentiation (Figure 1e, upper panel) in the absence of any additional osteogenic signals. IL-17 (50 ng/ml) was as potent as BMP-2 (30 ng/ml) in inducing osteogenic differentiation of primary hMSCs during a 10-day culture (data not shown). The ability of IL-17 to induce osteoblastic differentiation of hMSCs was further confirmed by the dramatically enhanced mineralization of IL-17-treated hMSCs (Figure 1e, lower panel). To exclude the possibility that the increased ALP activity was simply due to increased proliferation, we cultured hMSCs in the presence of 10 μM 5-azacytidine, which completely blocked IL-17-induced proliferation (Supplementary Figure 3c). The IL-17-dependent increase in the ALP activity was still observed when hMSCs were cultured in the presence of 5-azacytidine, suggesting that IL-17 stimulated the osteoblastic differentiation of hMSCs independent of its effect on proliferation (Figure 1f). The incubation of hMSCs with IL-17 for 24 h resulted in increased expression of ALP, Runx2, and Cox2 mRNA, further confirming that IL-17 can induce osteoblast differentiation from hMSCs (Figure 1g). Next, we used a Boyden chamber assay to test whether IL-17 can induce migration of hMSCs toward a IL-17 gradient (Figure 1h). Primary hMSCs were added to the upper chamber followed by the addition of IL-17 into the lower chamber. At 8 h after incubation, a significantly higher number of hMSCs was recovered from the lower chamber, suggesting that hMSCs migrate towards IL-17. Finally, the effect of IL-17 on the motility of primary hMSCs was tested by a wound-healing assay (Figure 1i). A greater number of hMSCs moved into the wound site after a 24-h incubation with IL-17, suggesting higher motility of hMSCs in the presence of IL-17. Migration and would-healing experiments with Cambrex MSCs produced similar results, further confirming that IL-17 can stimulate hMSC migration and motility (Supplementary Figure 4).Taken together, the data in Figure 1 suggest that IL-17 binding to IL-17 receptor(s) on the surface of hMSCs promotes their proliferation, differentiation, chemotaxis, and motility.

IL-17-stimulated generation of ROS in hMSCs is mediated by Nox1. The mechanism by which IL-17 induces proliferation of hMSCs has never been explored. ROS seem to be involved in the proliferation of fibroblasts[16] and several other types of mammalian cells.[17] To test whether the generation of ROS is involved in IL-17-dependent hMSC proliferation, we measured intracellular production of ROS in hMSCs after IL-17 treatment using 2′,7′-dichlorofluorescein-diacetate (DCFH-DA), an oxidation-sensitive fluorescent dye. IL-17 stimulated a rapid production of ROS in Cambrex MSCs (Figure 2a) as well as in primary hMSCs (Supplementary Figure 5), whereas the addition of an anti-oxidative agent, N-acetylcysteine (NAC), completely diminished the DCFH-DA fluorescence. Time course analysis showed significantly increased levels of ROS as early as 1 min after IL-17 stimulation; the maximum levels of ROS were observed at 10 min after treatment (Figure 2b). Furthermore, addition of a neutralizing anti-IL-17Ra antibody markedly attenuated the generation of ROS on IL-17 stimulation. We next investigated the signaling pathways downstream of IL-17-induced ROS generation. Treatment of hMSCs with IL-17 resulted in increased phosphorylation of Akt, MEK, ERK, p38, and IκB (Figure 2c). The IL-17-dependent activation of MEK, ERK, and IκB was significantly attenuated in the presence of NAC, whereas that of p38 and Akt was not affected. NADPH oxidase (Nox) enzymes play an important role in the generation of ROS by producing superoxides.[18] As antioxidants attenuated IL-17-dependent signaling in hMSCs, we examined whether Nox enzymes were involved. The GTPase Rac1 can stimulate at least two of the Nox proteins, namely, Nox1 and Nox3.[19–21] Upon IL-17 stimulation of hMSCs, there was a rapid increase in the levels of GTP-bound Rac1 (Figure 2d). At 5 min after IL-17

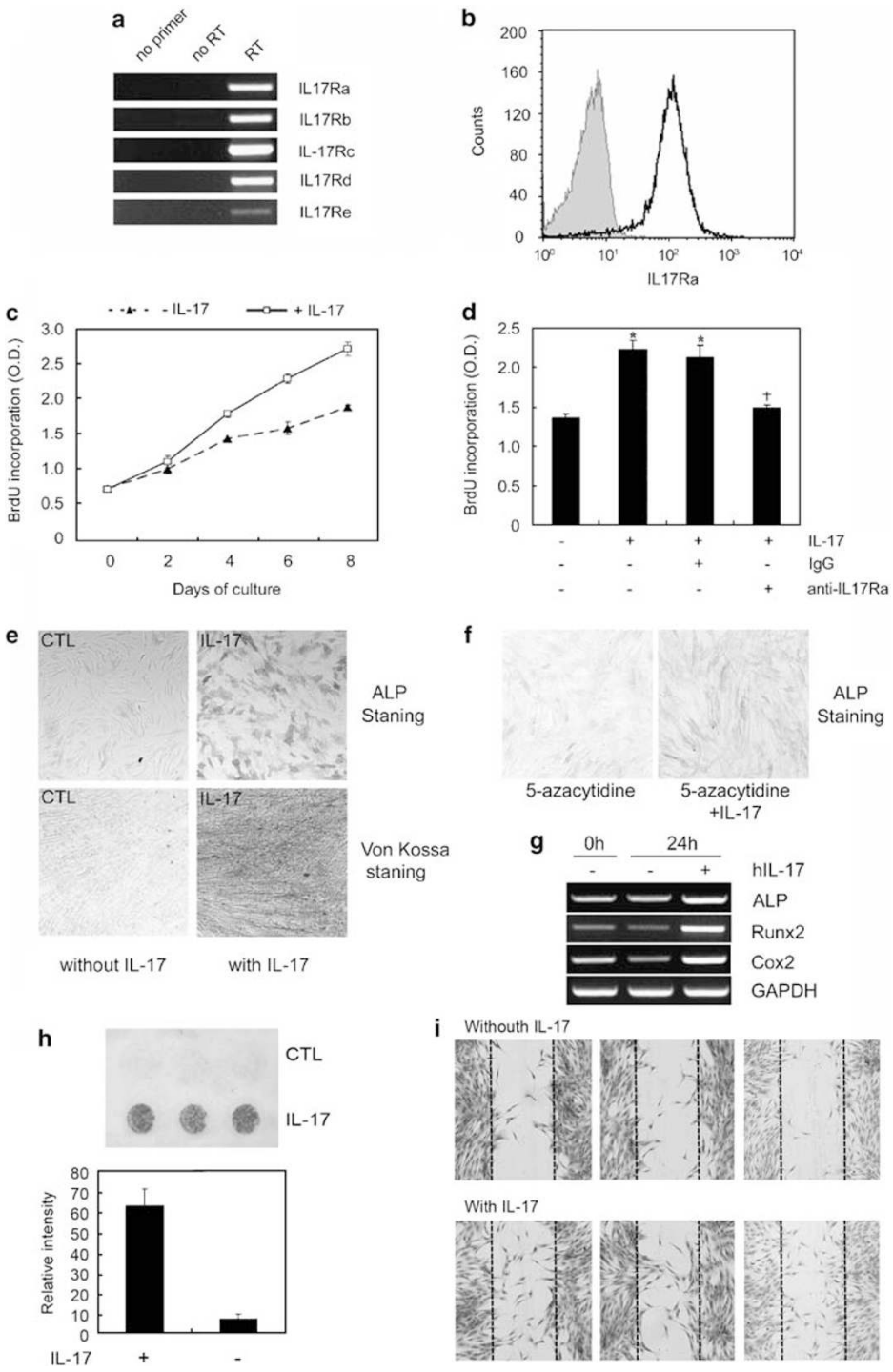

Figure 1 IL-17 induces hMSC proliferation, osteoblastic differentiation, chemotaxis, and motility. (**a**) The mRNA expression of IL-17 receptor family members in Cambrex MSCs was analyzed by RT-PCR. (**b**) The surface expression of IL-17Ra on Cambrex MSCs was analyzed by FACS. The gray line indicates the histogram obtained with an isotype control antibody. (**c**) The proliferation of Cambrex MSCs was determined by measuring BrdU incorporation after culturing the cells for 8 days with 50 ng/ml IL-17. (**d**) The effect of IL-17Ra neutralization on Cambrex MSC proliferation was determined by culturing the cells for 6 days with 50 ng/ml IL-17 in the presence of control IgG or anti-IL17Ra antibody (3 μg/ml). $^{*}P<0.05$ compared with untreated control. $^{\dagger}P<0.05$ compared with IL-17-treated sample. (**e**) The osteoblastic differentiation of Cambrex MSCs was determined by alkaline phosphatase (ALP) staining at 4 days after IL-17 (50 ng/ml) stimulation (upper panel). Mineralization was measured by von Kossa staining after a 26-day culture (lower panel). (**f**) The osteoblastic differentiation of Cambrex MSCs was determined by ALP staining in the presence of 50 ng/ml IL-17 and a proliferation inhibitor, 5-azacytidine (10 μM), for 4 days. (**g**) The mRNA expression of osteoblast markers in Cambrex MSCs was analyzed by RT-PCR after 24 h stimulation with 50 ng/ml IL-17. (**h**) The effect of IL-17 on primary hMSC migration was measured by a Boyden chamber assay. IL-17 (200 ng/ml) was added to the lower chamber. After an 8-h incubation, cells that were attached to the lower surface of the filter were stained and photographed. The relative density of migrated cells is shown in the histogram. (**i**) The effect of IL-17 on the motility of primary hMSCs was measured by observing the number of cells that moved into the wound site after a 24-h stimulation with 50 ng/ml IL-17. Photographs of triplicate samples are presented

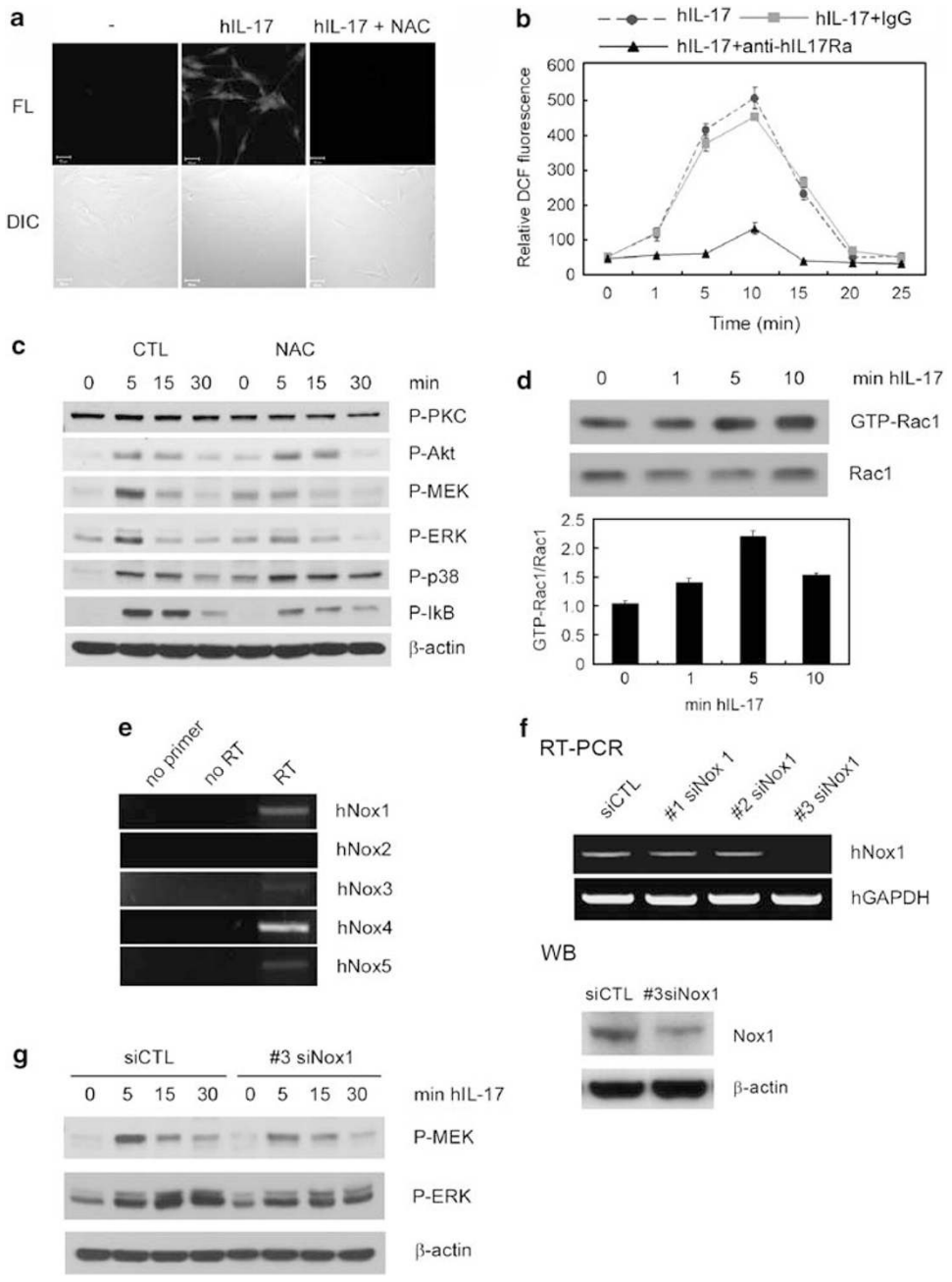

Figure 2 IL-17 stimulates ROS generation in hMSCs. (**a**) Cambrex MSCs were stimulated with recombinant IL-17 (200 ng/ml) for 10 min after pretreatment with vehicle or NAC (20 mM) for 1 h. The generation of ROS was measured by fluorescence confocal microscopy after DCFH-DA loading for 5 min. (**b**) Cambrex MSCs were pretreated with control IgG or anti-IL17Ra for 1 h and stimulated with IL-17 for the indicated times. The intracellular levels of ROS were measured and are expressed as relative fluorescence intensities. (**c**) Control or NAC (20 mM, 1 h)-pretreated Cambrex MSCs were stimulated with IL-17 (100 ng/ml) for the indicated times. Phosphorylated PKC, Akt, MEK, ERK, p38, and IκB were detected by western blot analyses. (**d**) Cambrex MSCs were stimulated with IL-17 (100 ng/ml) for the indicated times. The level of GTP-Rac1 was determined as described in Materials and Methods. (**e**) The mRNA expression of Nox family members in hMSCs was analyzed by RT-PCR. (**f**) Cambrex MSCs were infected with retroviruses harboring three Nox1 siRNA constructs. The knockdown of Nox1 mRNA and protein expression was examined by RT-PCR and western blotting. (**g**) The activation of MEK and ERK by IL-17 (100 ng/ml) were determined by western blotting in control or Nox1 knocked down Cambrex MSCs

stimulation, the amount of GTP-bound Rac1 was twofold greater than that in the absence of IL-17 (Figure 2d, lower panel). An RT-PCR analysis showed that hMSCs expressed Nox1 and Nox4 and, to a lesser extent, Nox3 and Nox5, whereas the expression of Nox2 was undetectable (Figure 2e). These results led us to hypothesize that a Rac-dependent Nox protein is involved in the generation of ROS and downstream signaling on IL-17 stimulation of hMSCs. We tested this hypothesis by downregulating Nox1 utilizing small interfering RNA (siRNA). By infecting hMSCs with retroviruses harboring Nox1-targeting sequences, we were able to suppress the mRNA and protein expression of

Nox1 (#3 siNox1, Figure 2f). The other two viruses (#1 siNox1 and #2 siNox1) were ineffective and were therefore used as controls in further experiments. Compared with control cells infected with viruses expressing siRNA targeted against luciferase (siCTL), Nox1 downregulated hMSCs (#3 siNox1) exhibited reduced MEK and ERK activation on IL-17 stimulation (Figure 2g). Interestingly, although the levels of Nox4 mRNA expression were higher in hMSCs (Figure 2e), downregulation of Nox4 by siRNA affected neither MEK nor ERK activation, nor did it alter the IL-17-dependent proliferation of these cells (data not shown). In addition, a flavoprotein-dependent oxidase inhibitor, diphenyleneiodonium (DPI), strongly blocked IL-17-induced ROS generation in hMSCs, supporting the role of Nox in IL-17-stimulated ROS production (Supplementary Figure 5). Taken together, these results indicate that Nox1 plays a role in IL-17-induced generation of ROS and downstream signaling in hMSCs.

TRAF6 and Act1 mediate IL-17-dependent generation of ROS. We next investigated which signaling molecules upstream of Nox1 are activated in hMSCs on IL-17 stimulation. Schwandner *et al*.[22] suggested that TRAF6 might directly bind to the IL-17 receptor, thereby mediating the cellular functions of IL-17 in mouse embryonic fibroblasts. Furthermore, Act1 was recently shown to associate with both TRAF6 and the IL-17 receptor in fibroblasts.[23] To examine the roles of TRAF6 and Act1 in IL-17-dependent signaling, we first examined the expression of these two proteins in hMSCs. As shown in Figure 3a, hMSCs express mRNA for both TRAF6 and Act1. To investigate the functions of TRAF6 and Act1 during IL-7-induced proliferation of hMSCs, we knocked down their expression using retrovirus-mediated siRNA. Infection of hMSCs with viruses harboring specific siRNA target sequences resulted in hMSCs with significantly lower mRNA and protein expression of TRAF6 (#2 siTRAF6) and Act1 (#2 siAct1) (Figure 3b). Figure 3c shows that the IL-17-dependent activation of MEK was significantly impaired in TRAF6 or Act1 knocked down hMSCs compared with cells infected with viruses harboring luciferase-targeting sequences (siCTL) or ineffective siRNA constructs (#1 siTRAF6 and #1 siAct1). Moreover, the amount of GTP-bound Rac1 was also significantly lower in IL-17-treated hMSCs when TRAF6 or Act1 expression was knocked down (Figure 3d). In addition, the silencing of TRAF6 or Act1 in hMSCs significantly decreased IL-17-induced ROS production detected by DCFH-DA fluorescence (Figure 3e). Taken together, these results suggest that TRAF6 and Act1 are crucial upstream signaling components of IL-17-stimulated ROS production.

Roles of TRAF6, Act1, and Nox1 in IL-17 stimulated proliferation of hMSCs. We next examined the role of IL-17-dependent signaling pathways in IL-17-induced hMSC proliferation. The knockdown of TRAF6 or Act1 in hMSCs almost completely attenuated IL-17-induced proliferation, as examined by BrdU incorporation into these cells (Figure 4a). Similarly, knockdown of Nox1 by retroviral infection reduced the IL-17-dependent proliferation of hMSCs (Figure 4b, #3 siNox1), whereas viruses ineffective at decreasing the Nox1 levels (#1 siNox1 and #2 siNox1) showed no such effect. Furthermore, the Nox inhibitor DPI, which strongly abrogates ROS generation, blocked IL-17-induced proliferation of hMSCs (Figure 4c and Supplementary Figure 3a). NAC treatment consistently resulted in the complete inhibition of IL-17-stimulated hMSC proliferation (Figure 4d and Supplementary Figure 3a). Finally, pharmacological inhibition of MEK, ERK, and NF-κB pathways hampered IL-17-dependent proliferation of hMSCs (Figure 4e). Although the MEK inhibitor, U0126, most strongly impaired the IL-17-induced proliferation of hMSC, the IKK inhibitor and phosphatidylinositol 3-kinase inhibitor, LY294002, also impaired IL-17-induced hMSC proliferation, albeit to a lesser extent. In contrast, the inhibition of the IL-17-activated p38 pathway, which was independent of ROS generation (Figure 2c), did not affect IL-17-induced proliferation of hMSCs. IL-17 did not stimulate ALP activity in the presence of NAC, suggesting that ROS generation is also involved in the IL-17-induced osteoblastic differentiation of hMSCs (Figure 4f).

M-CSF indirectly stimulates the secretion of IL-17 by T cells in PBMC culture. We next sought to determine the source of IL-17 in the bone microenvironment. In a preliminary microarray experiment, we discovered that the expression of IL-17 was significantly increased when human peripheral blood mononuclear cells (PBMCs) were cultured with M-CSF and RANKL to induce osteoclast differentiation. However, we later found out that it was M-CSF, not RANKL, which actually induced IL-17 production (Figure 5a, and data not shown). During the 9-day culture period, significant amounts of IL-17 were detected in the culture supernatants of PBMCs stimulated with M-CSF, regardless of the presence of RANKL. In contrast, PBMC-derived macrophages generated by culturing PBMCs with M-CSF for 3 days did not produce IL-17, excluding PBMC-derived macrophages as the source of IL-17. We next tested whether T cells, presumably T_H-17 cells, produce IL-17.[7] As shown in Figure 5b, among freshly isolated human PBMCs, only a small proportion of T cells were positive for IL-17. However, on culture with M-CSF, there was a marked increase in the number of T cells expressing IL-17. Again, there was no significant difference in the IL-17-positive T-cell population in the presence or absence of RANKL. We next tested whether M-CSF directly stimulates IL-17 expression on T cells or indirectly triggers the production of IL-17-positive T cells by supporting macrophage–T cell interactions. To this end, T cells and monocytes/macrophages were purified from PBMC with CD3 and CD14 antibody-conjugated microbeads, respectively. The purity of monocytes/macrophages and T cells reached 99 and 93%, respectively (Figure 5c, top and middle panels). Macrophages derived from the purified monocytes by incubation with M-CSF were cocultured with T cells in the presence of M-CSF. The production of IL-17 was markedly stimulated by M-CSF in cocultures of purified T cells and macrophages (Figure 5c, bottom panel). In sharp contrast, IL-17 production was close to basal levels when purified T cells were treated with M-CSF in the absence of macrophages, suggesting that M-CSF does not directly stimulate IL-17 production by T cells. Finally, the M-CSF-

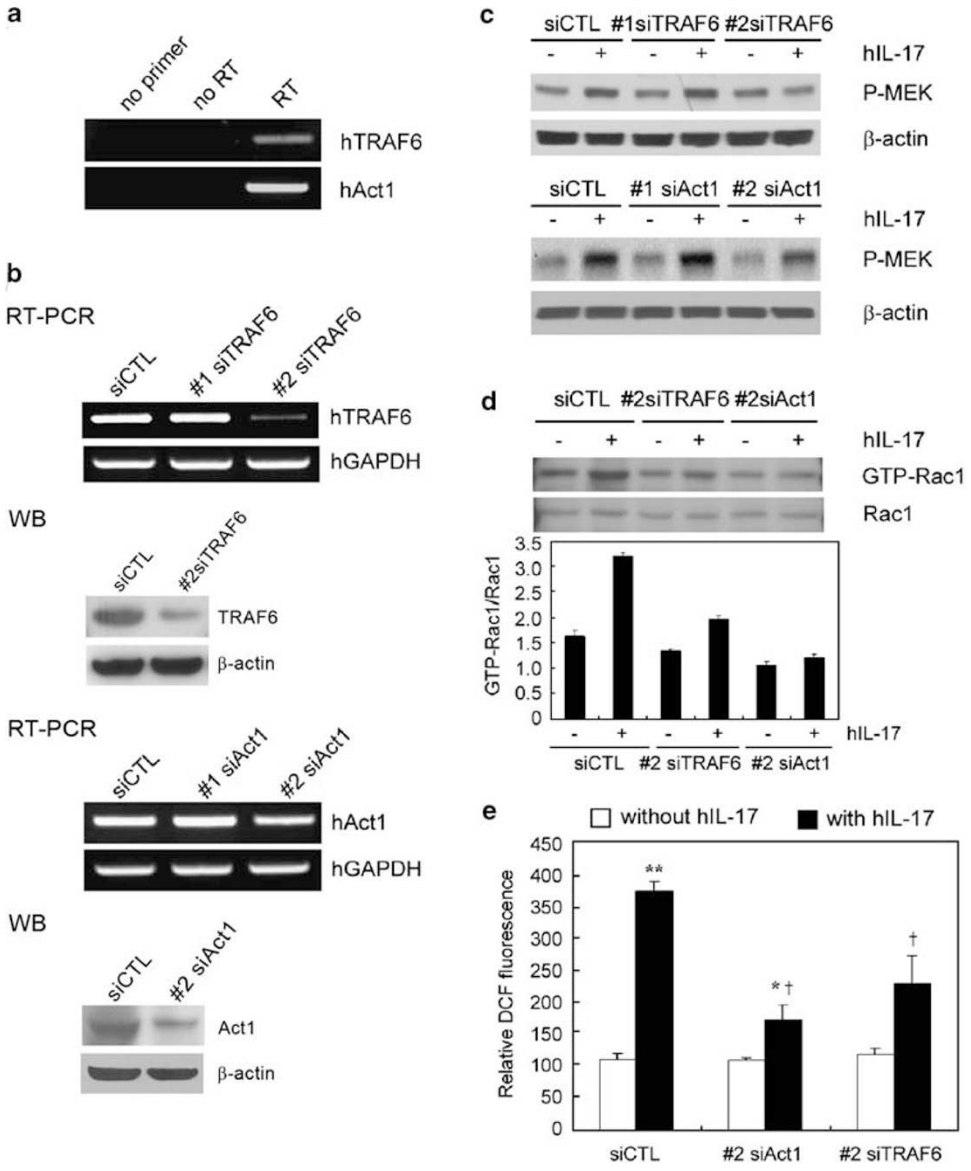

Figure 3 TRAF6 and Act1 mediate IL-17-induced ROS generation. (**a**) The mRNA expression of TRAF6 and Act1 was determined by RT-PCR in Cambrex MSCs. (**b**) Cambrex MSCs were infected with retroviruses harboring siRNA constructs targeting TRAF6 and Act1. The specific reduction of TRAF6 and Act1 mRNA and protein expression was determined by RT-PCR and western blotting. (**c**) The activation of MEK by IL-17 (100 ng/ml, 5 min) was determined in control, TRAF6 (#1 siTRAF6, inactive; #2 siTRAF6, active), and Act1 (#1 siAct1, inactive; #2 siAct1, active) knocked down Cambrex MSCs by western blotting. (**d**) The level of GTP-Rac1 after IL-17 stimulation (100 ng/ml, 10 min) was determined in control, TRAF6, and Act1 knocked down Cambrex MSCs. (**e**) The generation of ROS by IL-17 was measured in control, TRAF6, and Act1 knocked down Cambrex MSCs. siRNA oligonucleotides were used instead of retroviruses as described in the Materials and Methods. $^{**}P<0.01$ and $^{*}P<0.05$ compared with IL-17-untreated control. $^{\dagger}P<0.05$ compared with IL-17-treated siCTL sample

dependent IL-17 production in T cell–macrophage coculture was abrogated when T cells were not in contact with macrophages (separated by Transwell membrane), suggesting that direct contact between T cells and macrophages is required for the production of IL-17. Furthermore, the culture supernatants of T cell–macrophage cocultures induced hMSC proliferation significantly; this proliferation was blocked by the addition of anti-IL-17 neutralizing antibody (Figure 5d).

IL-17 stimulates osteoclastogenesis in the presence of MSCs. It has been established that osteoblasts support osteoclastogenesis by expressing RANKL. As IL-17 stimulated osteoblastic differentiation of hMSCs, we tested whether IL-17-treated hMSCs could augment osteoclastogenesis. PBMCs were induced to differentiate into osteoclasts in the presence of hMSCs together with IL-17, M-CSF, or M-CSF plus RANKL. When PBMCs were cocultured with hMSCs, IL-17 alone induced the generation of TRAP-positive osteoclastic cells at a level higher than observed when M-CSF was used (Figure 6a). In the absence of hMSCs, IL-17 did not increase the TRAP-positive population compared with the efficient generation of TRAP-positive cells by M-CSF or M-CSF plus RANKL

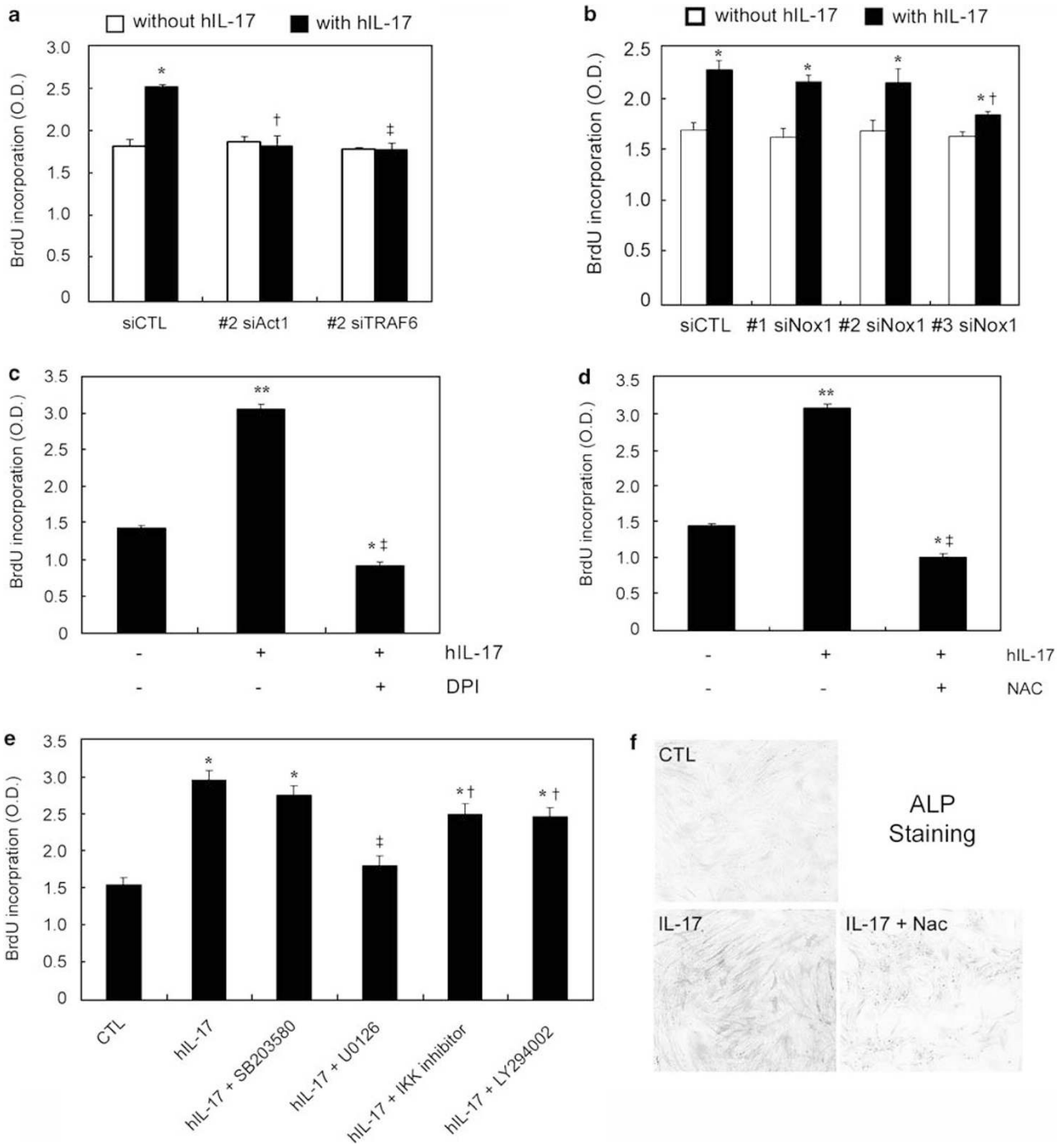

Figure 4 Role of IL-17-dependent signaling pathways in hMSC proliferation and differentiation. (**a**) Cell proliferation in the presence or absence of IL-17 (50 ng/ml, 6 days) was determined in control, TRAF6, and Act1 knocked down Cambrex MSCs by BrdU incorporation assays. (**b**) Cambrex MSCs were infected with Nox1 siRNA viruses (#1 and #2 siNox1, inactive; #3 siNox1, active). Cell proliferation was measured by BrdU incorporation. (**c** and **d**) Cambrex MSCs were cultured with IL-17 (50 ng/ml) for 6 days in the presence of vehicle, DPI (100 nM), or NAC (20 mM). Cell proliferation was measured by BrdU incorporation. (**e**) The proliferation of Cambrex MSCs was determined after treatment with IL-17 (50 ng/ml) for 6 days in the presence of SB203580 (10 μM), U0126 (1 μM), IKK inhibitor (1 μM), or LY294002 (1 μM). (**f**) Cambrex MSCs were cultured with 50 ng/ml IL-17 in the presence or absence of NAC (20 mM) for 4 days. Osteoblastic differentiation was determined by ALP staining. $^{**}P<0.01$ and $^{*}P<0.05$ compared with IL-17-untreated control sample. $^{\ddagger}P<0.01$ and $^{\dagger}P<0.05$ compared with IL-17-treated control sample

(Supplementary Figure 6). IL-17 stimulation not only induced osteoblastic differentiation of hMSCs, but also promoted the rapid induction of M-CSF and RANKL expression in primary hMSCs (Figure 6b). To further test whether IL-17 induces osteoclast differentiation *in vivo*, we implanted collagen matrices containing IL-17 and hMSCs into mice calvaria. Staining of calvarium sections for TRAP activity showed that IL-17 in combination with hMSCs induced the formation of

TRAP-positive osteoclasts *in vivo* (Figure 6c). Similarly, enhanced osteoclastogenesis was observed when the mouse calvarium was cultured *ex vivo* in the presence of IL-17 and hMSCs (data not shown). Figure 6d summarizes our findings that macrophages stimulate the generation of IL-17 from T_H-17 cells, which in turn induces the proliferation, chemotaxis, motility, and osteoblastic differentiation of hMSCs. The osteoblasts differentiated from hMSCs, in the presence of IL-17, accelerate the differentiation of osteoclasts. In addition, IL-17 stimulates the production of M-CSF and RANKL by hMSCs, thereby supporting macrophages and osteoclasts.

Discussion

The current understanding of the interaction between hMSCs and T-cell immunology is that hMSCs have immunosuppressive effect on T cells both *in vitro* and *in vivo*.[24,25] However, the effects of T cells and T-cell cytokines on the regulation of hMSC function have rarely been studied. As the regulation of bone homeostasis by T cells is of great interest, we explored the effect of the T-cell cytokine IL-17 on the function of MSCs that can differentiate into osteoblasts. IL-17, secreted primarily by T_H-17 cells, induces tissue inflammation. IL-17 has been shown to induce the proliferation of cells of various origins such as endometrial stromal cells and airway epithelial cells.[26,27] Notably, Huang *et al*.[15] reported that IL-17 might stimulate the formation of fibroblast-like colonies from human bone marrow stromal cells, suggesting a putative role of IL-17 in stimulating hMSC proliferation. However, these authors did not clearly define the identity of the stromal cells, leaving open the question as to whether IL-17 might directly stimulate the proliferation of hMSCs. Furthermore, the IL-17-dependent signaling pathways responsible for IL-17-dependent hMSC proliferation were unknown. In this study, we used human bone marrow-derived MSCs (both primary hMSCs and commercially-available Cambrex MSCs). We evaluated their ability to differentiate into adipocytes, chondrocytes, and osteoblasts (Supplementary Figure 1), and determined which surface markers they expressed (Supplementary Figure 2) to clearly show that IL-17 can stimulate the proliferation of defined hMSCs. The regulation of hMSC proliferation by IL-17 was of particular interest, because we observed high levels of expression and secretion of IL-17 by T cells in the presence of macrophages (Figure 5). Indeed, the bone microenvironment, especially in rheumatoid arthritis synovium, is rich in T cells and monocyte/macrophages with an ample amount of M-CSF present, suggesting that IL-17 may regulate MSC function. Although the precise mechanism by which macrophages stimulate the generation of T_H-17 cells remains to be elucidated by further studies, the requirement for direct contact between T cells and macrophages (Figure 5c) suggests that cell surface proteins, not soluble factors, are involved in this process.

In this report, we provided clear evidence that IL-17 stimulates the proliferation and osteoblastic differentiation of hMSCs (Figure 1). The mechanism by which IL-17 stimulates these hMSC responses was proven to involve the generation of ROS (Figure 2). Addition of IL-17 to hMSCs induced the rapid generation of ROS, whereas incubation of cells with anti-oxidative agents completely blocked the IL-17-dependent proliferation and differentiation of hMSCs (Figure 4). However, the effect of IL-17 on osteoblastic differentiation of hMSCs is separate from its effect on their proliferation, as IL-17 could stimulate osteoblastic differentiation when proliferation was inhibited by 5-azacytidine (Figure 1f). This divergence implies that IL-17 may play different roles at different stages of osteoblastogenesis. The generation of ROS by IL-17 involved the activation of the Nox complex (Figure 2 and Supplementary Figure 5). Importantly, knockdown of Nox1 by siRNA prevented IL-17-induced proliferation, confirming the crucial involvement of this Nox enzyme. Furthermore, TRAF6 and Act1 were critical for the activation of the Nox complex, as evidenced by the lack of IL-17-dependent Rac1 activation and proliferation of hMSCs in the absence of TRAF6 and Act1 (Figures 3 and 4). The MEK-ERK kinases are suggested as downstream target of ROS formed on IL-17 stimulation (Figure 2). Unlike published results suggesting the crucial involvement of TAK1 in mediating IL-17 signaling in human airway epithelial cells and mouse embryonic fibroblasts,[28,29] we did not observe any difference in the IL-17-dependent activation of MEK and ERK in hMSCs overexpressing dominant-negative (DN) TAK1 (Supplementary Figure 7). Rather, MEK and ERK were hyperphosphorylated by IL-17 in the presence of DN TAK1. Further studies should follow to determine whether the kinase activity of TAK1 or the adaptor-like role of TAK1 is important for IL-17-dependent signaling in hMSCs. Taken together, our results clearly show that IL-17 stimulates the proliferation of hMSCs through the generation of ROS by TRAF6 and Act1-dependent activation of the Nox complex, and ultimately, the activation of MEK-ERK kinases.

In terms of the coupling of bone formation and bone resorption, osteoblasts express both M-CSF and RANKL on their surface, which are the two pivotal cytokines required for osteoclastogenesis.[12,30] Among many human diseases associated with abnormal IL-17 levels, rheumatoid arthritis is of particular interest, because an earlier study revealed that IL-17 could induce the production of inflammatory cytokines from synovial fibroblasts.[31] In a later study, IL-17 was linked to osteoclast-mediated bone destruction; IL-17 stimulated RANKL expression on osteoblasts.[5] In addition, T_H-17 cells have been shown to have high levels of RANKL expression and directly stimulate osteoclastogenesis.[13] Thus, we extended our study to investigate whether IL-17 could regulate MSC function to induce osteoclastogenesis. In addition to stimulating proliferation, IL-17 also induced the motility and migration of hMSCs (Figure 1). Furthermore, IL-17 facilitated the expression of ALP and the formation of mineralized nodules by hMSCs, suggesting augmented osteoblast differentiation. Finally, IL-17-stimulated hMSCs expressed both M-CSF and RANKL, and showed enhanced osteoclast differentiation in the absence of exogenously added M-CSF and RANKL, both *in vitro* and *in vivo* (Figure 6). Until now, it has been suggested that osteoclastogenesis is favored in the presence of T_H-17 cells by both direct (stimulation of osteoclast precursors by RANKL on T_H-17 cells) and indirect (stimulation of osteoblasts by IL-17 produced by T_H-17 cells) mechanisms. Our results add to the current knowledge of T_H-17 cell function in the regulation of osteoclastogenesis by

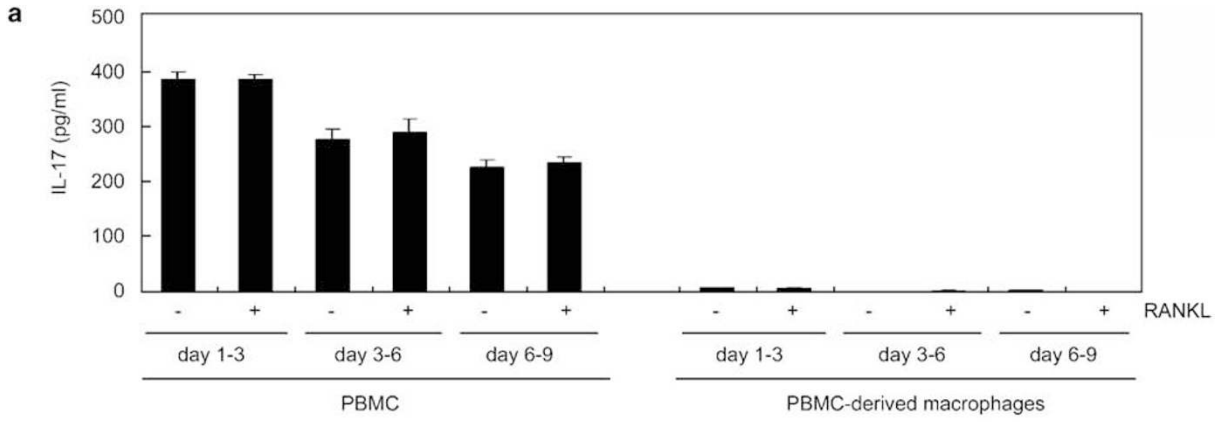
a
IL-17 (pg/ml)
500
400
300
200
100
0
- + - + - + - + - + - +
RANKL
day 1-3
day 3-6
day 6-9
day 1-3
day 3-6
day 6-9
PBMC
PBMC-derived macrophages

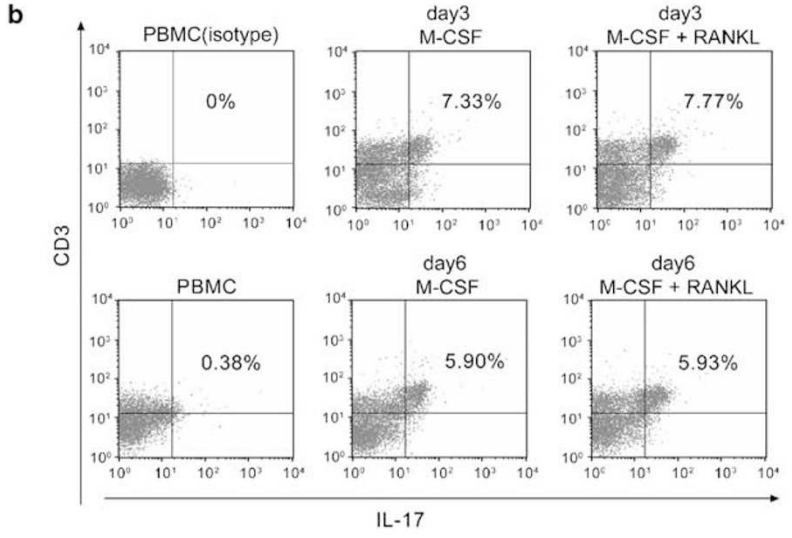
b
PBMC(isotype)
0%
day3
M-CSF
7.33%
day3
M-CSF + RANKL
7.77%
PBMC
0.38%
day6
M-CSF
5.90%
day6
M-CSF + RANKL
5.93%
CD3
IL-17

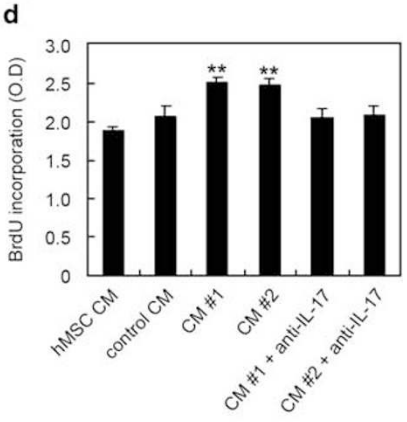
d
BrdU incorporation (O.D)
3.0
2.5
2.0
1.5
1.0
0.5
0
**
**
hMSC CM
control CM
CM #1
CM #2
CM #1 + anti-IL-17
CM #2 + anti-IL-17

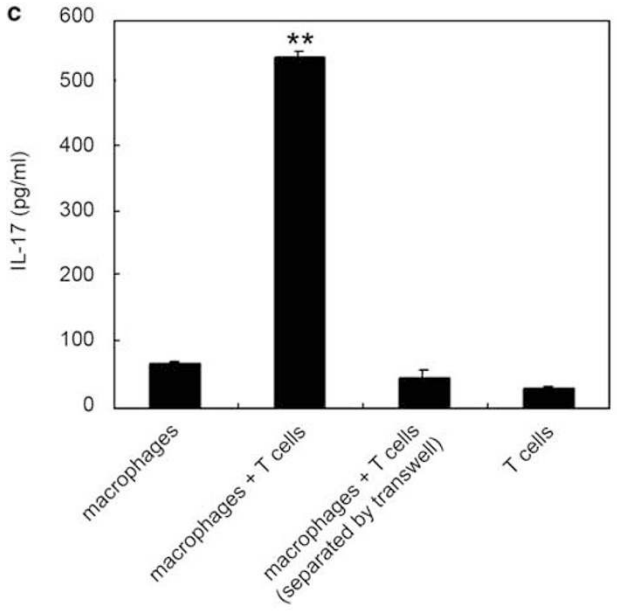
c
IL-17 (pg/ml)
600
500
400
300
200
100
0
**
macrophages
macrophages + T cells
macrophages + T cells
(separated by transwell)
T cells

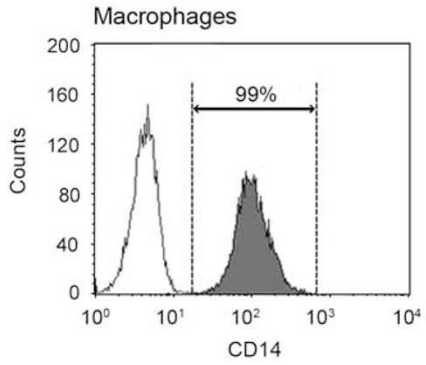
Macrophages
Counts
200
160
120
80
40
0
99%
10^0 10^1 10^2 10^3 10^4
CD14

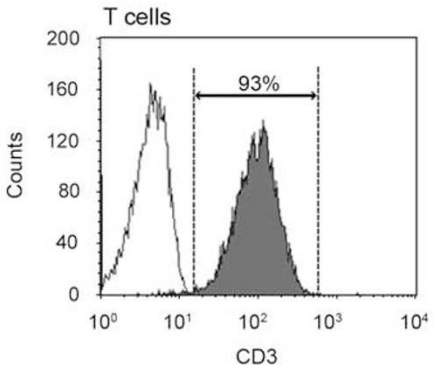
T cells
Counts
200
160
120
80
40
0
93%
10^0 10^1 10^2 10^3 10^4
CD3

suggesting a third mechanism by which IL-17 stimulates the proliferation, migration, and osteoblastic differentiation of MSCs. MSCs can be recruited and proliferate in a IL-17-high milieu. IL-17 can then induce the expression of M-CSF and RANKL on MSCs as well as on osteoblasts differentiated from MSCs, providing favorable conditions for osteoclastogenesis.

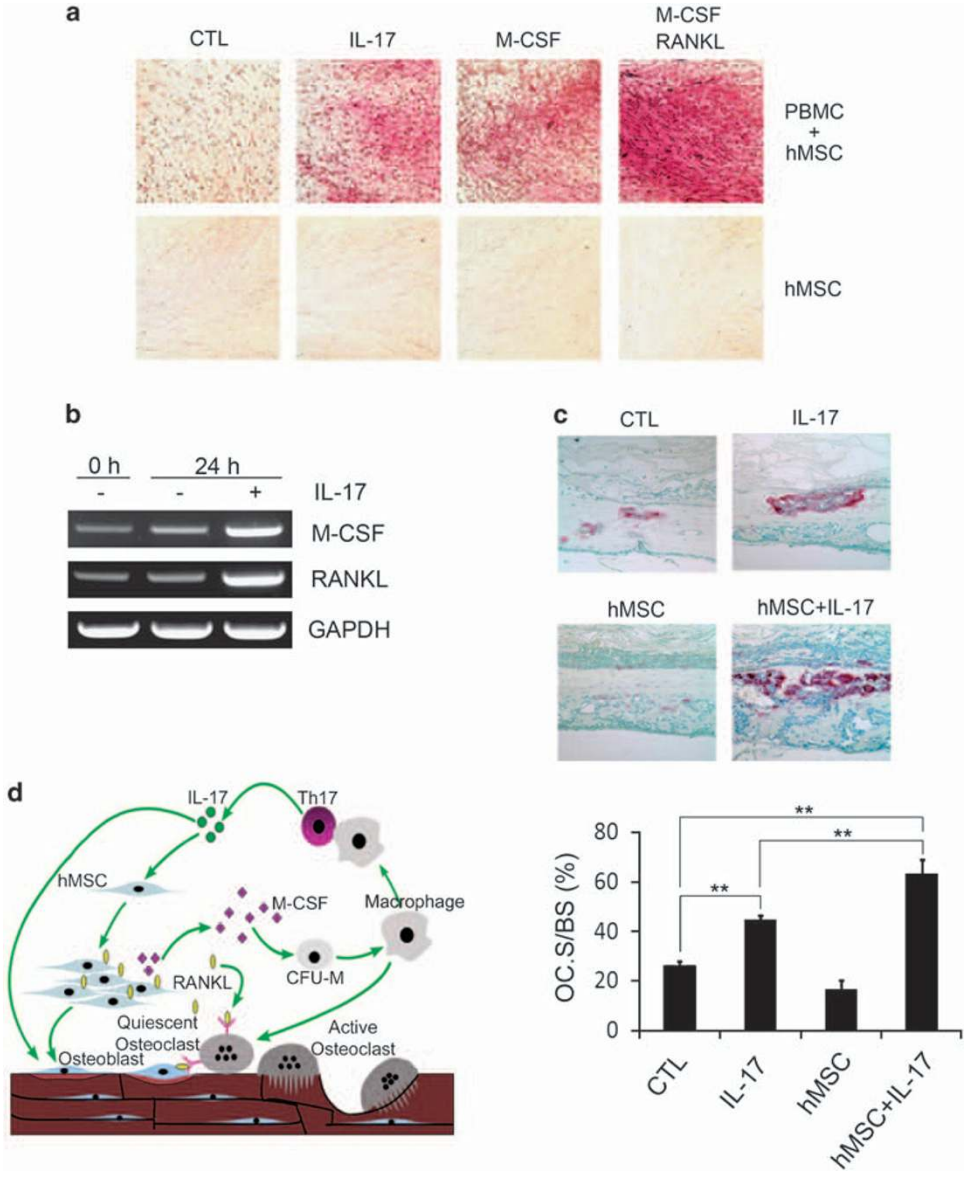

Figure 6 IL-17 regulation of hMSC function affects osteoclastogenesis. (**a**) Human PBMCs were cocultured with primary hMSCs in the presence of IL-17 (50 ng/ml), M-CSF (30 ng/ml), and RANKL (100 ng/ml) for 6 days. After fixing, cells were stained for TRAP activity to assess the formation of osteoclasts. (**b**) Primary hMSCs were cultured with IL-17 (50 ng/ml) for 24 h and the mRNA expression of M-CSF and RANKL was analyzed by RT-PCR. (**c**) Collagen disks loaded with IL-17 (20 ng) and primary hMSCs (2×10^6) were implanted onto mice calvaria. After 5 days, tissue sections (four mice per group) were prepared and stained for TRAP activity. The osteoclast surface and bone surface were measured using Spot Advanced software (Diagnostic Instruments). $^{**}P<0.01$ between indicated groups. (**d**) A schematic diagram summarizing the role of T-cell-derived IL-17 on the regulation of hMSC function and osteoclastogenesis

Figure 5 Generation of T_H-17 cells by coculture of macrophages with T cells. (**a**) Human PBMCs were cultured for 9 days with 100 ng/ml M-CSF in the absence or presence of RANKL (100 ng/ml). The levels of IL-17 protein in culture media collected within a 3-day interval were analyzed by ELISA. Alternatively, human PBMC-derived macrophages were cultured under the same condition as described above, and the IL-17 levels in the culture media were assessed by ELISA. (**b**) Human PBMCs were cultured with M-CSF (100 ng/ml) alone or M-CSF plus RANKL (100 ng/ml) for the indicated times and analyzed by FACS for the surface expression of CD3 and IL-17 after gating for lymphocytes. (**c**) Human monocytes and T cells were isolated using anti-CD14 and anti-CD3 beads as described in the Materials and Methods. The purity of isolated cells was determined by FACS analysis (top and middle panels). Macrophages derived from the purified monocytes were further cultured with purified T cells for 3 days in the presence of 100 ng/ml M-CSF. The amount of IL-17 in the culture media was analyzed by ELISA (bottom panel). (**d**) Primary hMSCs were treated with the culture media obtained in (**c**) for 12 days in the absence or presence of an IL-17 neutralizing antibody with media changes every 4 days. Cell proliferation was measured by BrdU incorporation. Control CM: supernatants of macrophage single cultures treated with M-CSF. CM#1 and CM#2: supernatants of M-CSF-treated cocultures of macrophages and T cells obtained from two different PBMC donors. $^{**}P<0.01$ compared with control CM

As hyper-osteoclastogenesis is frequently concomitant with bone destruction in inflamed sites, and because IL-17 seems to play a major role in inflammatory pathogenesis, including rheumatoid arthritis, we suggest that therapies targeting IL-17 may uncouple the osteoclastogenesis and osteoblastogenesis cycles and be effective candidates to treat inflammatory bone lytic diseases.

Materials and Methods

Regents. Recombinant human IL-17 was purchased from R&D Systems (Minneapolis, MN, USA). RANKL and M-CSF were obtained from PeproTech Inc. (Rocky Hill, NJ, USA). Lipofectamine 2000 was purchased from Invitrogen Life Technologies (Carlsbad, CA, USA). The reactive oxygen-dependent fluorescent dye DCFH-DA was purchased from Molecular Probes (Leiden, the Netherlands). Anti-human IL-17 and IL17Ra neutralizing antibodies were from R&D Systems. Anti-TRAF6 antibody was purchased from Stressgen (Ann Arbor, MI, USA). Phospho-specific antibodies against Akt, MEK, ERK, p38, JNK, and IκB were obtained from Cell Signaling Technology (Beverly, MA, USA). NAC was purchased from Sigma (St. Louis, MO, USA). Inhibitors U0126, SB203580, DPI, and LY294002 were obtained from Calbiochem (La Jolla, CA, USA). 5-Azacytidine was purchased from Sigma.

Cells. Commercially available human MSCs were purchased from Cambrex (Walkersville, MD, USA). Primary human MSCs were isolated from the patients' femur samples obtained during surgical operation. Briefly, bone marrow cells suspended in phosphate-buffered saline (PBS) were layered on lymphocyte separation medium (density 1.077 g/ml, Cellgro, Manassas, VA, USA) and centrifuged at 1100 $\times$ *g* for 30 min at 4°C. Cells collected from the interface were washed and resuspended in low glucose DMEM (Welgene, Daegu, Korea) supplemented with 10% fetal bovine serum (FBS) (Biowhittaker, Walkersville, MD, USA). After culture for 6 weeks, cells were tested for surface expression of MSC markers and differentiation into cells of mesenchymal origin. Human MSCs between passages 2 and 7 were used for all experiments. PBMCs were isolated from the peripheral blood of healthy donors. In some experiments, T cells and monocytes were purified from PBMCs using IMag anti-human CD3- and CD14-conjugated microbeads (BD Bioscience Pharmingen, San Diego, CA, USA), respectively. The purity of isolated cells was determined by FACS analyses. All experimental protocols were approved by the institutional research committee of Seoul National University.

Flow cytometry. To identify IL-17-producing cells, PBMCs were fixed with 2% formaldehyde, briefly permeabilized with 0.1% Triton X-100, and incubated with anti-human CD3 antibody (eBioscience, San Diego, CA, USA; 1 : 400) followed by fluorescein isothiocyanate-labeled anti-mouse IgG (Sigma; 1 : 1000) and anti-IL-17 (Santa Cruz Biotechnology, Santa Cruz, CA, USA; 200 : 1) followed by Cy3-conjugated anti-rabbit IgG (Jackson ImmunoResearch, West Grove, PA, USA; 1 : 1000), respectively. Fluorescence was measured with FACS Calibur (Becton Dickinson, Franklin Lakes, NJ, USA) and analyzed with Cell Quest software (Becton Dickinson).

IL-17 ELISA and transwell experiments. PBMCs (2×10^6/well in 48-well plates) were grown in α-MEM supplemented with 10% FBS. PBMC-derived macrophages (adherent cells obtained by treating PBMCs with 30 ng/ml M-CSF for 3 days) were seeded at 10^6/well in 48-well plates. After addition of 30 ng/ml M-CSF and 100 ng/ml RANKL, culture supernatants were collected every 3 days. The amount of IL-17 in culture supernatants was measured by enzyme-linked immunosorbent assay (ELISA) according to the manufacturer's instructions (R&D Systems). Alternatively, T cells and monocytes purified with anti-CD3 and anti-CD14 microbeads, respectively, were used. Purified T cells (10^6/well) were cocultured with macrophages derived from the purified monocytes (10^6/well) in the presence of M-CSF (30 ng/ml). In transwell experiments, macrophages were seeded in bottom plate wells and T cells were added onto the 5 μm pore insert of the transwell-24 system (Corning, Lowell, MA, USA). After 3 days, culture media were collected and IL-17 levels were measured by ELISA.

Cell proliferation and Rac1 activity assay. Proliferation of hMSCs was measured by quantification of BrdU incorporation into S-phase cells using a QIA58 BrdU ELISA kit (Calbiochem). Activation of Rac1 was determined using an EZ-Detect Rac1 activation kit (Pierce, Rockford, IL, USA) and 500 μg of cell lysate.

Assay of intracellular ROS. Human MSCs were cultured on 4.5-μm thick cover glasses in 6-well plates. After serum starvation for 5 h, cells were stimulated with IL-17, washed with DMEM lacking phenol red, and incubated for 5 min in Krebs-Ringer solution (Sigma-Aldrich) containing 10 μM DCFH-DA in the dark. The cover glass on which stimulated hMSCs were attached was transferred to a Zeiss LSM 5 Pascal confocal microscope (Carl Zeiss, Thornwood, NY, USA), and DCF fluorescence was measured with an excitation wavelength of 488 nm and emission at 505–530 nm. To avoid photooxidation of DCF, the fluorescence image was collected by a single rapid scan (4-line average, total scan time of 4.5 s). After collection of the fluorescence image, the mean relative fluorescence intensity for each group of cells was measured using Zeiss LSM 5 Pascal software.

Vector-based siRNA preparation and retroviral gene transfer. For siRNA experiments, 21 base oligonucleotide target sequences were ligated into pSuper-retro vector (Oligoengine, Seattle, WA, USA) using BamHI and HindIII sites as previously described.[32] VSV-G pseudotyped retroviruses were generated by transfecting HEK cells with pEQ-PAM3-E, pSRa-VSV-G, and pSuper-retro-Nox1siRNA, pSuper-retro-TRAF6siRNA, or pSuper-retro-Act1siRNA plasmids. The conditioned medium was harvested and filtered through a 0.45-μm filter after 48 h. Retroviral infection was performed by incubating hMSCs with VSV-G pseudotyped retrovirus-containing supernatant with the addition of 6 μg/ml polybrene for 48 h. Successful infection of cells was monitored by detecting GFP fluorescence. The target sequences to generate siRNA vector for each gene are listed in the Supplementary Table 2.

Oligonucleotide-mediated RNA interference. To knock down the levels of endogenous TRAF6 and Act1 protein, hMSCs were transfected with double-stranded RNA oligonucleotides at a final concentration of 20 nM using lipofectamin 2000 according to the manufacturer's instructions. After a 36-h incubation, the intracellular ROS levels of cells were analyzed. The target sequences used to generate the RNA interference oligonucleotides for each gene are listed in the Supplementary Table 3.

RT-PCR. One μg of total RNA was heated to 65°C for 10 min followed by chilling on ice. The denatured RNA was reverse transcribed in the presence of 0.5 μg of poly dT in 20 μl buffer containing 1 mM dNTP, 25 mM Tris–HCl, 50 mM KCl, 2 mM DTT, 5 mM $MgCl_2$, 1 U of RNase inhibitor, and 20 U of SuperScript II reverse transcriptase (Invitrogen). The mixture was incubated for 50 min at 42°C and for 15 min at 70°C. One μl of the generated cDNA was used for PCR with the thermal cycles of denaturing at 94°C, annealing at 55–60°C, and extension at 72°C for 30 s each. The number of amplification cycles was determined to be in a linear range of amplification, that is, 22 cycles for GAPDH and 25–30 cycles for the others. The primer sequences are listed in the Supplementary Table 1.

Western blotting analysis. Western blotting experiments were carried out as previously described.[33] Briefly, cells were washed twice with ice-cold PBS and ruptured with lysis buffer containing 20 mM Tris–HCl, 150 mM NaCl, 1% Triton X-100, and protease and phosphatase inhibitors. Cell extracts were microcentrifuged for 20 min at 10 000 $\times$ *g* and supernatants were collected. In all 30 μg of cellular protein was resolved by SDS-PAGE and transferred onto PVDF membranes. Membranes were blocked for 1 h with 5% skim milk in Tris-buffered saline containing 0.1% Tween 20 and incubated overnight at 4°C with primary antibodies. Membranes were washed, incubated for 1 h with appropriate secondary antibodies conjugated to horseradish peroxidase, and developed using chemiluminescence substrates.

Migration and wound healing assay. A Boyden chamber was used to assess the migration of MSCs through polycarbonate filters (pore size 8.0 μm). 2×10^6 hMSCs in 56 μl DMEM (low glucose) were placed in the upper wells. The lower wells of the chamber were loaded with 28 μl of DMEM with IL-17 (100 ng/ml). At 8 h after incubation, cells that had migrated to the lower surface of the filter were fixed and stained with Hemacolor for Microscopy kit (Merck, Darmstadt, Germany). Images were obtained using a UMAX powerlook1100 scanner (UMAX, Taipei, Taiwan). Human MSC monolayers were wounded by scratching with a pipette tip. After washing the debris, hMSCs were treated with IL-17 (50 ng/ml) for 24 h. Cells were fixed with 3.7% formaldehyde solution, stained with hematoxylin solution

(Sigma-Aldrich), and observed using an Olympus BX51 microscope (Olympus, Center Valley, PA, USA) equipped with a Spot Insight digital camera system (Diagnostic Instruments, Sterling Heights, MI, USA). To measure cell densities, images were analyzed by densitometry using the Image J (http://rsbweb.nih.gov/ij/) program.

Osteoblastic differentiation. Human MSCs were cultured in α-MEM supplemented with 10% FBS containing 20 ng/ml IL-17. ALP staining was performed to examine osteoblast differentiation using the ALP staining kit (Sigma-Aldrich) according to the manufacturer's instructions. For the detection of mineralized nodules, hMSCs were stained by the von Kossa staining method. Stained cells were observed using an Olympus BX51 microscope.

hMSC-PBMC coculture. Human MSCs (10^4/well) were seeded on 48-well plates in α-MEM containing 10% FBS. After overnight adherence, human PBMCs (5×10^5 cells) were added to each well and cultured in the presence or absence of IL-17 (50 ng/ml), M-CSF (30 ng/ml), and RANKL (100 ng/ml). After 6 days, osteoclasts were stained for TRAP activity using a Leukocyte Acid Phosphatase Kit (Sigma).

***In vivo* stimulation of osteoclastogenesis by hMSC and IL-17.** Collagen disks (10 mm diameter, 0.5 mm thickness) loaded with 20 ng IL-17 and 2×10^6 primary hMSCs were implanted onto mice calvariae. After 5 days, calvariae were removed, fixed, and decalcified before paraffin embedding. Tissue sections of 5 μm thickness were stained for TRAP activity to examine osteoclastogenesis.

Statistical anaysis. Data are represented as mean $\pm$ S.D. Groups were compared by the two-tailed Student's *t*-test or one-way ANOVA with Student–Newman-Keuls *post hoc* tests (Figure 6c). Differences with $P < 0.05$ were regarded as significant.

Acknowledgements. We thank Dr. In Sook Kim and Ms. Tae Hyung Cho for their help with the *in vivo* experiments. This work was supported by grants from the 21C Frontier Functional Proteomics Project (FPR08B1-170), the Research Program for New Drug Target Discovery (M10748000257-07N4800-25710), and the Science Research Center (R11-2008-023-01001-0); all projects funded by the Korea Science & Engineering Foundation, Ministry of Education, Science and Technology, Korea.

Conflict of interest

The authors declare no conflict of interest.

1. Kolls JK, Linden A. Interleukin-17 family members and inflammation. *Immunity* 2004; **21**: 467–476.
2. Kawaguchi M, Adachi M, Oda N, Kokubu F, Huang SK. IL-17 cytokine family. *J Allergy Clin Immunol* 2004; **114**: 1265–1273; quiz 1274.
3. Wong CK, Ho CY, Li EK, Lam CW. Elevation of proinflammatory cytokine (IL-18, IL-17, IL-12) and Th2 cytokine (IL-4) concentrations in patients with systemic lupus erythematosus. *Lupus* 2000; **9**: 589–593.
4. Wong CK, Ho CY, Ko FW, Chan CH, Ho AS, Hui DS *et al.* Proinflammatory cytokines (IL-17, IL-6, IL-18 and IL-12) and Th cytokines (IFN-gamma, IL-4, IL-10 and IL-13) in patients with allergic asthma. *Clin Exp Immunol* 2001; **125**: 177–183.
5. Kotake S, Udagawa N, Takahashi N, Matsuzaki K, Itoh K, Ishiyama S *et al.* IL-17 in synovial fluids from patients with rheumatoid arthritis is a potent stimulator of osteoclastogenesis. *J Clin Invest* 1999; **103**: 1345–1352.
6. Antonysamy MA, Fanslow WC, Fu F, Li W, Qian S, Troutt AB *et al.* Evidence for a role of IL-17 in organ allograft rejection: IL-17 promotes the functional differentiation of dendritic cell progenitors. *J Immunol* 1999; **162**: 577–584.
7. Langrish CL, Chen Y, Blumenschein WM, Mattson J, Basham B, Sedgwick JD *et al.* IL-23 drives a pathogenic T cell population that induces autoimmune inflammation. *J Exp Med* 2005; **201**: 233–240.
8. Yao Z, Painter SL, Fanslow WC, Ulrich D, Macduff BM, Spriggs MK *et al.* Human IL-17: a novel cytokine derived from T cells. *J Immunol* 1995; **155**: 5483–5486.
9. Shin HC, Benbernou N, Esnault S, Guenounou M. Expression of IL-17 in human memory CD45RO+ T lymphocytes and its regulation by protein kinase A pathway. *Cytokine* 1999; **11**: 257–266.
10. Ferretti S, Bonneau O, Dubois GR, Jones CE, Trifilieff A. IL-17, produced by lymphocytes and neutrophils, is necessary for lipopolysaccharide-induced airway neutrophilia: IL-15 as a possible trigger. *J Immunol* 2003; **170**: 2106–2112.
11. Molet S, Hamid Q, Davoine F, Nutku E, Taha R, Page N *et al.* IL-17 is increased in asthmatic airways and induces human bronchial fibroblasts to produce cytokines. *J Allergy Clin Immunol* 2001; **108**: 430–438.
12. Teitelbaum SL, Ross FP. Genetic regulation of osteoclast development and function. *Nat Rev Genet* 2003; **4**: 638–649.
13. Sato K, Suematsu A, Okamoto K, Yamaguchi A, Morishita Y, Kadono Y *et al.* Th17 functions as an osteoclastogenic helper T cell subset that links T cell activation and bone destruction. *J Exp Med* 2006; **203**: 2673–2682.
14. Pittenger MF, Mackay AM, Beck SC, Jaiswal RK, Douglas R, Mosca JD *et al.* Multilineage potential of adult human mesenchymal stem cells. *Science* 1999; **284**: 143–147.
15. Huang W, La Russa V, Alzoubi A, Schwarzenberger P. Interleukin-17A: a T-cell-derived growth factor for murine and human mesenchymal stem cells. *Stem Cells* 2006; **24**: 1512–1518.
16. Murrell GA, Francis MJ, Bromley L. Modulation of fibroblast proliferation by oxygen free radicals. *Biochem J* 1990; **265**: 659–665.
17. Burdon RH. Superoxide and hydrogen peroxide in relation to mammalian cell proliferation. *Free Radic Biol Med* 1995; **18**: 775–794.
18. Lambeth JD. NOX enzymes and the biology of reactive oxygen. *Nat Rev Immunol* 2004; **4**: 181–189.
19. Ueyama T, Geiszt M, Leto TL. Involvement of Rac1 in activation of multicomponent Nox1- and Nox3-based NADPH oxidases. *Mol Cell Biol* 2006; **26**: 2160–2174.
20. Cheng G, Diebold BA, Hughes Y, Lambeth JD. Nox1-dependent reactive oxygen generation is regulated by Rac1. *J Biol Chem* 2006; **281**: 17718–17726.
21. Miyano K, Ueno N, Takeya R, Sumimoto H. Direct involvement of the small GTPase Rac in activation of the superoxide-producing NADPH oxidase Nox1. *J Biol Chem* 2006; **281**: 21857–21868.
22. Schwandner R, Yamaguchi K, Cao Z. Requirement of tumor necrosis factor receptor-associated factor (TRAF)6 in interleukin 17 signal transduction. *J Exp Med* 2000; **191**: 1233–1240.
23. Chang SH, Park H, Dong C. Act1 adaptor protein is an immediate and essential signaling component of interleukin-17 receptor. *J Biol Chem* 2006; **281**: 35603–35607.
24. Nauta AJ, Fibbe WE. Immunomodulatory properties of mesenchymal stromal cells. *Blood* 2007; **110**: 3499–3506.
25. Rasmusson I. Immune modulation by mesenchymal stem cells. *Exp Cell Res* 2006; **312**: 2169–2179.
26. Hirata T, Osuga Y, Hamasaki K, Yoshino O, Ito M, Hasegawa A *et al.* Interleukin (IL)-17A stimulates IL-8 secretion, cyclooxygensase-2 expression, and cell proliferation of endometriotic stromal cells. *Endocrinology* 2008; **149**: 1260–1267.
27. Inoue D, Numasaki M, Watanabe M, Kubo H, Sasaki T, Yasuda H *et al.* IL-17A promotes the growth of airway epithelial cells through ERK-dependent signaling pathway. *Biochem Biophys Res Commun* 2006; **347**: 852–858.
28. Huang F, Kao CY, Wachi S, Thai P, Ryu J, Wu R. Requirement for both JAK-mediated PI3K signaling and ACT1/TRAF6/TAK1-dependent NF-kappaB activation by IL-17A in enhancing cytokine expression in human airway epithelial cells. *J Immunol* 2007; **179**: 6504–6513.
29. Qian Y, Liu C, Hartupee J, Altuntas CZ, Gulen MF, Jane-Wit D *et al.* The adaptor Act1 is required for interleukin 17-dependent signaling associated with autoimmune and inflammatory disease. *Nat Immunol* 2007; **8**: 247–256.
30. Boyle WJ, Simonet WS, Lacey DL. Osteoclast differentiation and activation. *Nature* 2003; **423**: 337–342.
31. Fossiez F, Djossou O, Chomarat P, Flores-Romo L, Ait-Yahia S, Maat C *et al.* T cell interleukin-17 induces stromal cells to produce proinflammatory and hematopoietic cytokines. *J Exp Med* 1996; **183**: 2593–2603.
32. Lee Y, Hyung SW, Jung HJ, Kim HJ, Staerk J, Constantinescu SN *et al.* The ubiquitin-mediated degradation of Jak1 modulates osteoclastogenesis by limiting interferon-beta-induced inhibitory signaling. *Blood* 2008; **111**: 885–893.
33. Ryu J, Kim HJ, Chang EJ, Huang H, Banno Y, Kim HH. Sphingosine 1-phosphate as a regulator of osteoclast differentiation and osteoclast-osteoblast coupling. *EMBO J* 2006; **25**: 5840–5851.

Supplementary Information accompanies the paper on Cell Death and Differentiation website (http://www.nature.com/cdd)